tvst

DOI: 10.1167/tvst.3.4.5

Article

Depth Resolved Differences After Corneal Crosslinking With and Without Epithelial Debridement Using Multimodal Imaging

Praveena Gupta[1], Best Anyama[2], Kert Edward[3,4], Kevin Wells[2], Massoud Motamedi[1,3], Bernard F. Godley[1], and Gracie Vargas[3]

[1] Department of Ophthalmology and Visual Sciences, University of Texas Medical Branch, Galveston, TX
[2] School of Medicine, University of Texas Medical Branch, Galveston, TX
[3] Advanced Bio-Optics Imaging Laboratory, Center for Biomedical Engineering, University of Texas Medical Branch, Galveston, TX
[4] Department of Physics, University of the West Indies, Mona Campus, Mona, Jamaica

Correspondence: Praveena Gupta, Department of Ophthalmology and Visual Sciences, University of Texas Medical Branch, 301 University Blvd, Galveston, TX 77555-1106, USA.
e-mail: prgupta@utmb.edu

Received: 06 March 2014
Accepted: 03 June 2014
Published: 6 August 2014

Keywords: riboflavin; collagen crosslinking; transepithelial crosslinking; cornea; second harmonic generation

Citation: Gupta P, Anyama B, Edward K. Depth resolved differences after corneal crosslinking with and without epithelial debridement using multimodal imaging. Tran Vis Sci Tech. 2014;3(4):5, http://tvstjournal.org/doi/full/10.1167/tvst.3.4.5, doi: 10.1167/tvst.3.4.5

Purpose: To quantitatively compare stromal collagen architecture and keratocyte viability between two methods of corneal crosslinking (CXL), one involving invasive epithelial debridement (standard riboflavin crosslinking) and the other by the modified method of riboflavin TRIS–ethylenediaminetetraacetic acid (riboflavin-TE) transepithelial crosslinking, which conserves epithelial layer, using multimodal imaging.

Methods: Corneas of fresh porcine globes were treated with standard or with riboflavin-TE crosslinking for 30 minutes under a 370-nm ultraviolet A (UVA) light source (3 mW/cm^2). Depth resolved imaging by confocal and second harmonic generation (SHG) microscopy was performed after live/dead cell labeling. Evaluation of apoptotic keratocyte number and texture analysis based on surface roughness was performed on confocal and SHG image stacks, respectively.

Results: Surface texture and visual grading indicated significant alterations in stromal architecture following standard CXL compared with untreated controls, while riboflavin-TE CXL induced subtle alterations confined near the corneal surface. The standard CXL had a statistically lower ($P < 0.05$) average surface roughness (9.46 $\pm$ 2.8 AU), with no significant difference between controls (12.85 $\pm$ 2.96 AU) and riboflavin-TE CXL (14.34 $\pm$ 1.85 AU). Both CXL groups resulted in apoptotic keratocytes, differing significantly from controls, with 56.5% greater numbers of apoptotic cells in the standard CXL group than the TE-CXL group ($P < 0.05$).

Conclusion: Standard CXL produced significant architectural changes of the deeper stroma and caused increased collateral damage on the keratocytes in comparison to the riboflavin-TE CXL at all depths studied.

Translational Relevance: Multimodal imaging guided surface architectural analysis provided insights into the actual collagen changes that occur after CXL and may guide in real-time modifications of the CXL methods for effective therapeutic CXL.

Introduction

Keratoconus is a disorder in which the cornea progressively deforms into a conical shape causing various degrees of visual impairment. The disease results from the alterations in the anterior lamellar structure of the cornea, thus weakening the mechanical strength of the stroma leading to protrusion and scarring.[1,2] Conventional treatment modalities include rigid gas-permeable contact lens, intracorneal rings, and penetrating keratoplasty. In the last decade, collagen crosslinking (CXL) has emerged as a new treatment modality for keratoconus and is used as a first line of treatment in many countries outside United States. CXL has gained quick popularity due to its promising results in reducing the rate of disease progression and preservation of visual acuity.[3,4]

CXL increases the stiffness of the corneal stroma thus arresting further progression of keratoconus,[4–6] but not in all cases. Briefly, the standard CXL procedure involves de-epithelialization of the central zone followed by treatment with a photopolymerizing agent (0.1% riboflavin) under an ultraviolet A (UVA) lamp emitting 3 mW/cm^2 irradiance for 30 minutes. Long-term effects after the procedure are promising[5] and are clinically proven to slow or halt progression of keratoconus.[6,7] However, the debridement of the epithelium causes haze, increases the risk of corneal infection, and scarring leading to postoperative discomfort.[7,8] CXL also leads to apoptosis of keratocytes in the stroma, which may contribute to delay in vision recovery.[9,10]

More recently, transepithelial CXL with "epithelium-on" procedures have been proposed in an attempt to abate these adverse effects of standard CXL. Surface epithelial cells of the cornea act as a tight barrier for the penetration of the photopolymerizing agent into the corneal stroma. Therefore, in the transepithelial CXL method, collagen CXL is achieved by using permeability enhancers on the epithelial surface of the central cornea. Various transepithelial agents such as benzalkonium chloride, surfactants (TRIS), ethylenediaminetetraacetic acid (EDTA), and topical anesthetics have been shown to weaken the epithelial cell junctions, thus increasing penetration.[11–14] Clinically, the most widely used transepithelial CXL agent is riboflavin-dextran solution supplemented with TRIS-hydroxymethyl aminomethane and sodium EDTA (Ricrolin TE™; Sooft, Montegiorgio, Italy) that acts as permeabilizing/carriers for the polymerizing agent.[13,14] Filippello and coworkers[15] have clinically demonstrated the ability of Ricrolin TE transepithelial CXL to halt the progression of keratoconus for up to 18 months with improvement in visual acuity and topographic measurements. However, a recent study on keratoconic patients 26 years and younger, treated with "epithelium-on" Ricrolin TE transepithelial CXL showed deterioration and unstable outcomes at 24 months of assessment,[16] indicating there is a need to elucidate the factors, which contribute differences in outcomes between CXL approaches. A thorough in depth quantitative comparison is lacking as to what happens to the surface architectural features and associated collateral keratocyte damage between the traditional and the aforementioned method of CXL. In general, there is a need for methods, which can be used to evaluate cell viability and stromal microarchitecture for comparison of CXL techniques both in the short and long term. Such methods could be used to investigate and optimize dosing, efficacy, and outcomes of various CXL techniques.

Depth-resolved optical microscopy is an attractive choice for noninvasive study of microarchitecture and cytology of the cornea due to the ability to visualize microstructures with subcellular resolution and potentially to hundreds of microns in depth. The nonlinear optical microscopy method of second harmonic generation (SHG) provides contrast unique to fibrillar collagen in the cornea and has been applied to reveal differences in the lamellar organization between normal and keratoconus corneas.[2] Depth resolved fluorescence microscopy by confocal and multiphoton microscopy have provided the ability to assess cellular and stromal features and to evaluate spatial microstructural changes following CXL. Steven et al.,[17] demonstrated that nonlinear optical microscopy can be used to reveal morphometric differences in stromal architecture. They provided depth resolved qualitative information on the stromal changes post CXL within the treatment zone and outside the treatment zone showing CXL leads to visually altered backward SHG images.[17–20]

The use of SHG for assessment of corneal architectural change may be enhanced by the development of quantitative analyses and scoring methods that provide indication of degree of stromal change, as well as quantitative assessment of cell viability based on fluorescence. Thus, the current study aims to provide depth-resolved quantitative analysis of the surface architectural changes along with the induced collateral damage on the keratocytes due to effects of the standard CXL and the riboflavin TRIS-EDTA (riboflavin-TE) transepithelial CXL using SHG signal imaging and confocal microscopy. The importance of such a study lies in the fact that the recently developed riboflavin-TE method has garnered significant enthusiasm with early promising, but conflicting results as mentioned above. Such a study would not only provide a valuable assessment to clinical decision-making, but it may also help provide tools to optimize the CXL procedures for improved visual outcomes.

Methods

Eyes

Fresh porcine eyes were transferred from a local slaughter house at 4°C within 1 hour of death and were processed immediately for experiments. All specimens had clear corneas prior to the start of the

experiments. Globes were separated into three groups: nontreated control group ($n = 8$), standard CXL group ($n = 6$), and riboflavin-TE transepithelial CXL group ($n = 6$).

Crosslinking

Standard CXL procedure was performed using an established standard protocol.[21] The central zone of corneal epithelium was debrided with a diameter of 7 to 9 mm using a 10 mm scalpel blade. A 1-cm diameter rubber washer was placed on the cornea to prevent solution runoff while 0.1% riboflavin in 20% dextran solution was instilled with a dropper every 5 minutes for 30 minutes. Corneas were irradiated with UVA light at an irradiance of 3 mW/cm^2 using a UV spot curing system (EFOS Novacure, Mississauga, Ontario, Canada) and a band-pass filter centered at 370 nm ± 2 nm (Thorlabs, Newton, NJ). Corneas treated with riboflavin-TE transepithelial CXL were subjected to the same methods; however, the epithelium was not debrided and the aforementioned riboflavin solution was supplemented with TRIS-hydroxymethyl aminomethane and sodium EDTA. Control corneas were left untreated only to be moistened in phosphate buffered saline (PBS).

Staining

Following CXL procedures, corneas of the whole globe were stained with calcein-AM (Invitrogen, Molecular Probes/Invitrogen #C3099), a dye used to identify viable cells, and propidium iodide (PI) a dye used for detecting dying cells following CXL procedures. The standard CXL corneas that had been debrided in earlier steps were directly incubated in 1 μM calcein-AM and 1 μg/mL PI for 30 minutes. While the epithelium remained intact during CXL procedures, the epithelium was debrided from control and riboflavin-TE corneas to allow for penetration of dyes. All groups were washed thoroughly in PBS before imaging. The eye globes were used without any fixation or additional manipulation for live/dead cell staining prior to imaging.

Imaging Protocol

A combination of SHG and confocal microscopy was performed on the above mentioned treated and control corneas for contrast from fibrillar collagen (SHG) and the fluorescent stains of superficial lying cells (confocal). Images were captured using a modified Zeiss confocal laser scanning microscope (LSM 410; Zeiss, Oberkochen, Germany) allowing for SHG microscopy.[22] A near infrared femtosecond laser consisting of a Tsunami Ti:sapphire laser pumped by a frequency doubled Nd:YVO at 532 nm (Spectra Physics, Irvine, CA) served as the illumination source for SHG microscopy. The excitation source for confocal microscopy was an argon/krypton ion laser capable of providing 488, 568, and 647 nm illuminations. For SHG, 840 nm was used for illumination, resulting in production of a frequency-doubled (SHG) signal at 420 nm. SHG was collected using a 420 ± 20 nm filter. A 40× 0.8 numerical aperture water objective was used to capture images in the central corneal region of the epithelial debrided face. Images were obtained up to 300 μm in a z-stack using an interslice interval of 50 μm. Confocal microscopy was used to obtain fluorescent images of cells labeled with calcein-AM (excitation 488 nm, emission 500–550 nm) and PI (excitation 568 nm, emission long pass 590 nm), and SHG microscopy was used to capture signals from collagen to produce a profile image of corneal stromal architecture.

Histology

Following imaging, corneas were excised from the globes from each group and fixed in 10% formaldehyde for 48 to 72 hours. Slides were then prepared for hematoxylin and eosin (H&E) staining and imaged under a light microscope.

Image Processing

Apoptotic keratocytes were manually counted by a blinded observer with the assist of an image processing tool (ImageJ, National Institutes of Health, Bethesda, MD; available at http://rsb.info.nih.gov/ij/index.html). Corneal stromal architecture assessment of the SHG images from each group was performed using the ImageJ plug-in SurfCharJ, which provides an analysis of image texture features.[23] The SurfCharJ plug-in analyzed the roughness profile of the stromal architecture and generated root mean square deviation (Rq) values according to an international standardization texture parameter. Rq values determined for SHG images at multiple depths and values for corresponding depths were averaged within the groups. Preliminary examination of pilot training images indicated a loss in wavy pattern with CXL, which was moderate in riboflavin TE-CXL and enhanced in standard CXL. Based on these qualitative findings, a visual scoring system was applied to SHG images, with final scoring of the study images performed in a masked manner. Masked visual scoring of SHG images was applied

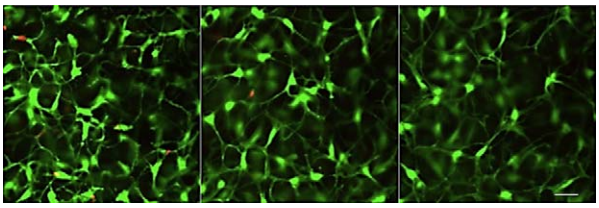

Figure 1. Representative images of keratocytes in an untreated control cornea stained with Calcein-AM (live cell marker, *green*) and PI (dead cell marker, *red*). Depth positions are (from left to right) 10, 20, and 50 μm from the surface after epithelium debridement. *Scale bar*, 10 μm.

using the following score metrics: 0 = form is smooth, flat, nondistinct; 1 = form is noticeable but with attenuated ruggedness/waviness; 2 = form is clearly distinct with pronounced ruggedness/waviness. Scored values were then averaged at corresponding depths within the groups. Ruggedness is defined in this study as having an irregular surface marked with wrinkle-like features.

Analysis

Statistical analysis of the averages between each group was accomplished using one- and two-way ANOVA with pairwise comparison. Data are presented as mean ± SEM with significance at P less than 0.05.

Results

Keratocyte Cell Death

Calcein-AM revealed a dense dendritic network of healthy keratocytes in the control corneas at various depths and a few positive PI-stained apoptotic cell nuclei localized near the anterior surface (Fig. 1). In contrast, apoptotic keratocytes were seen in all depths

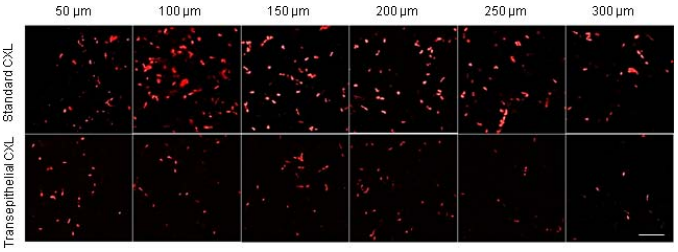

Figure 2. Images of apoptotic nuclei representing dead keratocytes (stained with Calcein-AM) in a porcine cornea treated with standard CXL (*upper panel*) and riboflavin-TE transepithelial CXL (*lower panel*). Depth positions are (from left to right) 50, 100, 150, 200, 250, and 300 μm from the surface. *Scale bar*, 30 μm.

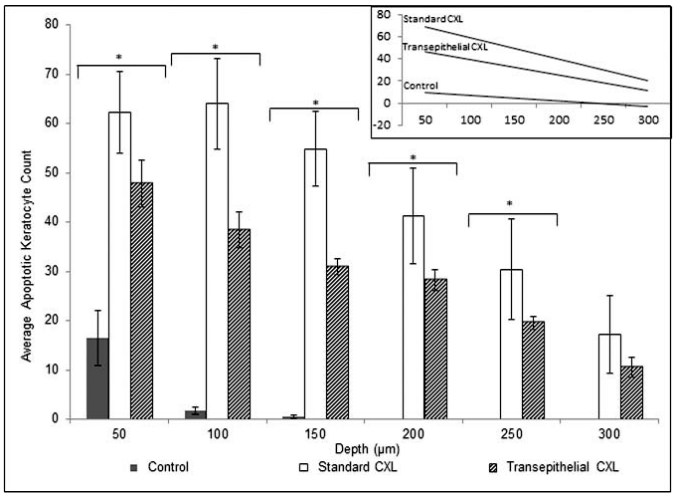

Figure 3. Average count of apoptotic keratocytes between the groups. Standard CXL slope value = −0.19; riboflavin-TE transepithelial CXL slope value = −0.14; control slope value = −0.05. Statistical significance at 50, 100, 150, 200, and 250 μm ($P < 0.05$); 300 μm ($P = 0.07$).

assessed (Fig. 2) in both the standard CXL and riboflavin-TE transepithelial CXL groups. With the exception of 300 μm, apoptotic keratocytes were significantly greater at every 50-μm depths intervals in the standard CXL than in riboflavin-TE transepithelial group as shown in Figure 3. The anterior most 50 μm revealed a 32% reduction in the apoptotic keratocytes in the riboflavin-TE transepithelial CXL group compared with the standard CXL group. This difference increased at deeper layers. Note that deeper tissues had less keratocyte deaths in both the groups. This is depicted in a linear regression graph (Fig. 3) by a negative slope (standard CXL, m = −0.19; riboflavin-TE transepithelial CXL, m = −0.14; control, m = −0.05). These results reflect the degree of

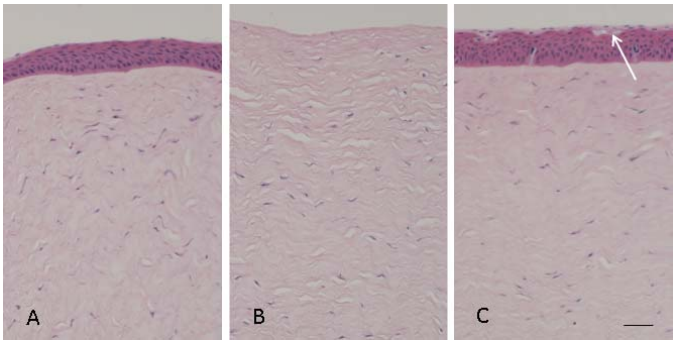

Figure 4. H&E-stained histological cross-section of (A) untreated control cornea, (B) standard CXL cornea, (C) riboflavin-TE transepithelial CXL cornea. *Arrow* represents apoptotic epithelial cells with disrupted cell junction. *Scale bar*, 50 μm.

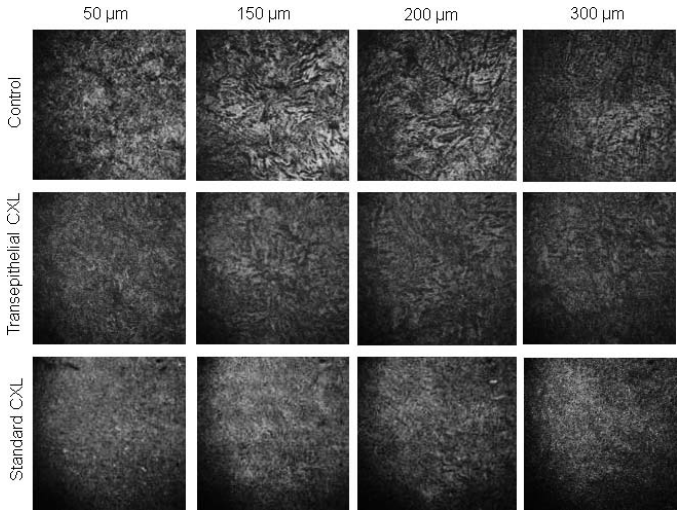

Figure 5. SHG images of corneal stroma in untreated control cornea (*upper panel*), in cornea treated with riboflavin-TE transepithelial CXL (*middle panel*), and in cornea treated with standard CXL (*lower panel*). Depth positions are (from left to right) 50, 150, 200, and 300 µm from the epithelial debrided surface. Note the smooth form profile in the standard CXL treatment as compared with untreated control and riboflavin-TE transepithelial corneas.

change in cell death with each method, the standard CXL method resulting in the most significant cell death followed by TE-CXL, with insignificant numbers in controls.

Histological Studies

Stromal architecture was visualized using standard H&E staining on a cross-section of cornea after standard and riboflavin-TE transepithelial CXL (Fig. 4). The anterior lamellae in the control cornea depicted a homogenous pattern with the keratocyte cell bodies interwoven in them. The standard CXL cornea demonstrated successful epithelium debridement, bundled collagen architecture, and few keratocytes. Also evident were de-novo pocket voids created by collagen fiber bundling. The riboflavin-TE transepithelial CXL cornea revealed apoptotic cell bodies in the surface epithelial layer characterized as balloon degeneration and chromatic condensation.

Stromal Architecture Assessment

Figure 5 compares a series of SHG images of corneal stroma between the three groups at all scanned depths. The control group displayed a rough surface with distinct waviness/ruggedness, which distinctly differed from the treatment groups in which the rugged/wavy pattern was attenuated. The riboflavin-TE transepithelial CXL group depicted noticeable ruggedness that was similar to the control group, albeit attenuated, and which extended to 150 µm in depth. Quantitative graphical representation of stromal architecture profile is displayed in Figures 6A and 6B. Standard CXL group had consistently lower average roughness Rq values at all depths when compared with control and riboflavin-TE transepithelial groups. Conversely, the riboflavin-TE transepithelial group had relatively similar Rq values to the control group. Visual scoring by a masked observer paralleled the results of roughness texture analysis (Figs. 6A–6C).

Discussion

SHG microscopy offers a promising method by which corneal morphology and effects of CXL on collagen can be assessed. Previous studies applying SHG for this application have shown qualitative differences in collagen architecture following CXL techniques. Additionally qualitative demonstration of decreased keratocyte population due to standard CXL has been shown through the use of two-photon autofluorescence.[17] Our goal in this study was to develop an approach for depth-dependent quantitative characterization of stromal architecture and keratocyte viability for the objective comparison between the traditional and transepithelial CXL approaches. Thus, we applied imaging by backscattered SHG and confocal fluorescence microscopy with live/dead cell fluorescent labels as a means to compare CXL approaches and applied quantitative scoring for objectively describing stromal architecture change and cell viability.

The use of live/dead cell markers with quantitation of keratocyte numbers as a function of depth allow for a specific measure of cell viability that autofluorescence alone cannot provide, thus providing objective measure of keratocyte death between CXL methods. In the current study, higher numbers of apoptotic keratocytes were quantified in the standard CXL groups than in the riboflavin-TE transepithelial CXL group, which displayed fewer apoptotic keratocytes in all the depths examined; while few/no apoptotic keratocytes were found in the control groups as expected (Fig. 3). These results are consistent with previous demonstration of significant loss of keratocytes near the surface of standard CXL corneas, assisted with nuclear staining of fixed corneal sections.[9,17,24] Since both CXL treatment groups in

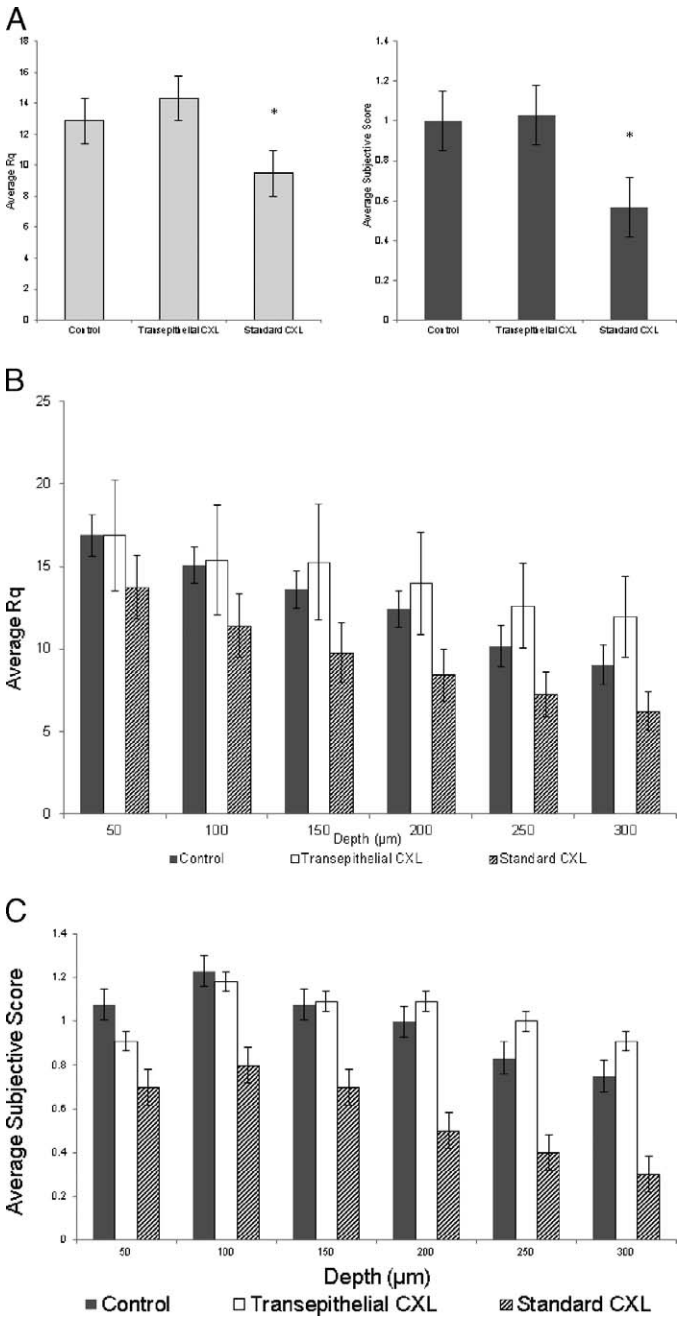

Figure 6. (A) Total average Rq values at all depths depicting the surface roughness (*left*) and average subjective score (*right*) of architecture of the stroma ($P < 0.05$). (B) Average Rq values of corneal stromal architecture at 50-μm depth intervals. There is a distinct decrease of Rq values in the standard CXL groups. 50 μm, $P = 0.56$; 100 μm, $P = 0.41$; 150 μm, $P = 0.27$; 200 μm, $P = 0.18$; 250 μm, $P = 0.15$; 300 μm, $P = 0.09$. (C) Subjective average score of corneal stromal architecture by a masked observer. 0 = smooth, flat, nondistinct; 1 = form is noticeable but with attenuated ruggedness; 2 = pronounced ruggedness.

the current study received equal irradiance, the difference in the apoptotic keratocytes in the riboflavin TE-CXL group is likely due to epithelial barrier that caused poor riboflavin penetration[25] and greater attenuation of UVA light into the deeper layers. In the standard CXL group, enhanced UVA and riboflavin cause the formation of reactive oxygen species, leading to additional covalent bonds between collagen molecules[6] and subsequently induce greater keratocyte apoptosis. Some degree of keratocyte death was noted up to 300 μm examined in this study, consistent with predictions of expected depths of apoptosis estimated from in vitro studies.[26] Similarly, UVA dose-dependent keratocyte damage has been shown on rabbit corneas using histological and transmission electron microscopy studies.[9] Because porcine corneas with epithelial layers are approximately 50-um thicker than the epithelium in humans, we expect that the numbers of apoptotic keratocytes may be slightly higher in clinical setting following riboflavin-TE transepithelial CXL than observed in the current study.

In addition to quantifying keratocyte death, in this study we introduced two quantitative image-based approaches by which the degree of stromal architecture change may be objectively described and applied acutely or long-term following CXL. The surface roughness analysis provides a method to compare the degree of texture change that is visually observed as a loss in waviness following CXL. Similar to our observations, Steven et al.,[17] showed loss of the wavelike pattern of collagen seen on control corneas, with CXL-corneas displaying homogeneous and smooth appearance within CXL zones compared with peripheral untreated regions. The standard CXL group consistently had lower average roughness Rq values when compared with the control and riboflavin-TE transepithelial CXL groups at their respective depths. An overall one-third less roughness was calculated in the standard CXL group based on the software. Both control and riboflavin-TE transepithelial groups exhibited relatively similar values. The average roughness Rq values correlated with the masked visual scoring (Figs. 6A–6C) suggesting validity and reproducibility of the assessment by SurfCharJ analysis. Though we report a correlation exists between the Rq values and amount of collagen crosslinking, further studies are warranted for quantitative measures on collagen crosslinking. Previous studies have provided objective measures of the corneal rigidity induced by the CXL using the stress-strain measures,[21,27–30] however, such studies

are conducted on excised corneas. The merit of the methods presented for image-based quantitation of roughness is that they may be developed for noninvasive and acute assessment of stromal architecture change for real time monitoring of the tissue crosslinking.

Corneal collagen CXL has been shown to induce corneal edema, and therefore the SHG imaging may show altered interlamellar architecture and nonuniform alterations.[31] The backward SHG patterns observed in the current study are similar to published reports.[18,32] The use of backward SHG imaging allows for noninvasive assessment of collagen architecture on corneas that is not possible with forward SHG requiring corneal extraction. Here, we show that despite increased noise in backward SHG definitive and significant quantitative differences in architecture occur between the CXL groups and controls (Fig. 5). In the future, it may be possible to develop backward SHG imaging as demonstrated here for long-term biomonitoring following in vivo clinical studies after CXL.

It is still a matter of debate on how much structural alterations are required to achieve long-term visual stability, but a desired CXL method should cause minimal collateral damage and maximum CXL effects. The methods presented here could be used to assess alterations in treatment parameters to assist in the development of a transepithelial approach with similar efficacy as standard CXL while maintaining an intact epithelium. For example, the methods could be used to assess parameter effects such as increasing the treatment time or riboflavin concentration, and/or UV irradiance. A recent study demonstrated that CXL is oxygen-dependent and that for enough CXL to happen, oxygen diffusion is necessary.[33] Therefore, in addition to the above mentioned modifiers oxygen diffusion time may also need to be standardized for optimum CXL.

In summary, methods for quantitative assessment of depth dependent stromal architectural change and keratocyte viability following CXL were presented. Studies conducted on ex vivo porcine eyes revealed that the standard CXL method caused greater alterations on collagen microarchitecture at depths up to 300 μm in comparison to the riboflavin-TE transepithelial CXL method. The number of apoptotic keratocytes were also higher in the standard CXL group at all depths studied, suggesting higher cytotoxic effects of the standard CXL method on the stroma and consistent with previous reports. While porcine cornea is an accepted model system for studying human cornea, ultrastructural stromal thickness differences may dictate altered results warranting future study in human cornea.

Acknowledgments

Supported in part by an unrestricted grant from Research to Prevent Blindness (RPB) to the University of Texas Medical Branch, Galveston, Texas, USA and R01 CA127429 from NIH to Gracie Vargas.

Disclosure: **P. Gupta**, None; **B. Anyama**, None; **K. Wells**, None; **K. Edward**, None; **G. Vargas**, None; **M. Motamedi**, None; **B. Godley**, None

References

1. Dhaliwal JS, Kaufman SC. Corneal collagen cross-linking: a confocal, electron, and light microscopy study of eye bank corneas. *Cornea*. 2009;28:62–67.
2. Morishige N, Takagi Y, Chikama T, Takahara A, Nishida T. Three-dimensional analysis of collagen lamellae in the anterior stroma of the human cornea visualized by second harmonic generation imaging microscopy. *Invest Ophthalmol Vis Sci*. 2011;52:911–915.
3. Jhanji V, Sharma N, Vajpayee RB. Management of keratoconus: current scenario. *Br J Ophthalmol* 2011;95:1044–1050.
4. Kampik D, Ralla B, Keller S, Hirschberg M, Friedl P, Geerling G. Influence of corneal collagen crosslinking with riboflavin and ultraviolet-a irradiation on excimer laser surgery. *Invest Ophthalmol Vis Sci*. 2010;51:3929–3934.
5. Wollensak G, Spoerl E, Seiler T. Riboflavin/ultraviolet-a-induced collagen crosslinking for the treatment of keratoconus. *Am J Ophthalmol*. 2003;135:620–627.
6. Raiskup F, Spoerl E. Corneal crosslinking with riboflavin and ultraviolet A. Part II. Clinical indications and results. *Ocul Surf*. 2013;11:93–108.
7. Kymionis GD, Portaliou DM, Bouzoukis DI, et al. Herpetic keratitis with iritis after corneal crosslinking with riboflavin and ultraviolet A for keratoconus. *J Cataract Refract Surg*. 2007;33:1982–1984.
8. Pollhammer M, Cursiefen C. Bacterial keratitis early after corneal crosslinking with riboflavin and ultraviolet-A. *J Cataract Refract Surg*. 2009;35:588–589.

9. Wollensak G, Spoerl E, Wilsch M, Seiler T. Keratocyte apoptosis after corneal collagen cross-linking using riboflavin/UVA treatment. *Cornea*. 2004;23:43–49.
10. Wollensak G, Iomdina E, Dittert DD, Herbst H. Wound healing in the rabbit cornea after corneal collagen cross-linking with riboflavin and UVA. *Cornea*. 2007;26:600–605.
11. Cha SH, Lee JS, Oum BS, Kim CD. Corneal epithelial cellular dysfunction from benzalkonium chloride (BAC) in vitro. *Clin Exp Ophthalmol*. 2004;32:180–184.
12. Kissner A, Spoerl E, Jung R, Spekl K, Pillunat LE, Raiskup F. Pharmacological modification of the epithelial permeability by benzalkonium chloride in UVA/Riboflavin corneal collagen cross-linking. *Curr Eye Res*. 2010;35:715–721.
13. Caporossi A, Mazzotta C, Baiocchi S, Caporossi T, Paradiso AL. Transepithelial corneal collagen crosslinking for keratoconus: qualitative investigation by in vivo HRT II confocal analysis. *Eur J Ophthalmol*. 2012;22(suppl 7);S81–S88.
14. Leccisotti A, Islam T. Transepithelial corneal collagen cross-linking in keratoconus. *J Refract Surg*. 2010;26:942–948.
15. Filippello M, Stagni E, O'Brart D. Transepithelial corneal collagen crosslinking: bilateral study. *J Cataract Refract Surg*. 2012;38:283–291.
16. Caporossi A, Mazzotta C, Paradiso AL, Baiocchi S, Marigliani D, Caporossi T. Transepithelial corneal collagen crosslinking for progressive keratoconus: 24-month clinical results. *J Cataract Refract Surg*. 2013;39:1157–1163.
17. Steven P, Hovakimyan M, Guthoff RF, Huttmann G, Stachs O. Imaging corneal crosslinking by autofluorescence 2-photon microscopy, second harmonic generation, and fluorescence lifetime measurements. *J Cataract Refract Surg*. 2010;36:2150–2159.
18. Bueno JM, Gualda EJ, Giakoumaki A, Perez-Merino P, Marcos S, Artal P. Multiphoton microscopy of ex vivo corneas after collagen cross-linking. *Invest Ophthalmol Vis Sci*. 2011;52:5325–5331.
19. Bottos KM, Dreyfuss JL, Regatieri CV, et al. Immunofluorescence confocal microscopy of porcine corneas following collagen cross-linking treatment with riboflavin and ultraviolet A. *J Refract Surg*. 2008;24:S715–S719.
20. Mazzotta C, Caporossi T, Denaro R, et al. Morphological and functional correlations in riboflavin UV A corneal collagen cross-linking for keratoconus. *Acta Ophthalmol (Copenh)*. 2012;90:259–265.
21. Wollensak G, Spoerl E, Seiler T. Riboflavin/ultraviolet-a-induced collagen crosslinking for the treatment of keratoconus. *Am J Ophthalmol*. 2003;135:620–627.
22. Edward K, Qiu S, Resto V, McCammon S, Vargas G. In vivo layer-resolved characterization of oral dysplasia via nonlinear optical microspectroscopy. *Biomed Opt Express*. 2012;3:1579–1593.
23. Chinga G, Johnsen P, Dougherty R, Berli EL, Walter J. Quantification of the 3D microstructure of SC surfaces. *J Microsc*. 2007;227:254–265.
24. Mencucci R, Marini M, Paladini I, et al. Effects of riboflavin/UVA corneal cross-linking on keratocytes and collagen fibres in human cornea. *Clin Exp Ophthalmol*. 2010;38:49–56.
25. Sondergaard AP, Hjortdal J, Breitenbach T, Ivarsen A. Corneal distribution of riboflavin prior to collagen cross-linking. *Curr Eye Res*. 2010;35:116–121.
26. Wollensak G, Spoerl E, Reber F, Seiler T. Keratocyte cytotoxicity of riboflavin/UVA-treatment in vitro. *Eye (Lond)*. 2004;18:718–722.
27. Wollensak G. Crosslinking treatment of progressive keratoconus: new hope. *Curr Opin Ophthalmol*. 2006;17:356–360.
28. Asri D, Touboul D, Fournie P, et al. Corneal collagen crosslinking in progressive keratoconus: multicenter results from the French National Reference Center for Keratoconus. *J Cataract Refract Surg*. 2011;37:2137–2143.
29. Bottos KM, Dreyfuss JL, Regatieri CV, et al. Immunofluorescence confocal microscopy of porcine corneas following collagen cross-linking treatment with riboflavin and ultraviolet A. *J Refract Surg*. 2008;24:S715–719.
30. Kymionis G, Portaliou D. Corneal crosslinking with riboflavin and UVA for the treatment of keratoconus. *J Cataract Refract Surg*. 2007;33:1143–1144, author reply 1144.
31. Hsueh CM, Lo W, Chen WL, et al. Structural characterization of edematous corneas by forward and backward second harmonic generation imaging. *Biophys J*. 2009;97:1198–1205.
32. Kruger A, Hovakimyan M, Ramirez Ojeda DF, et al. Combined nonlinear and femtosecond confocal laser-scanning microscopy of rabbit corneas after photochemical cross-linking. *Invest Ophthalmol Vis Sci*. 2011;52:4247–4255.
33. Richoz O, Hammer A, Tabibian D, Gatzioufas Z, Hafezi F. The biomechanical effect of corneal collagen cross-linking (CXL) with riboflavin and UV-A is oxygen dependent. *Transl Vis Sci Technol*. 2013;2:6.